Materials Physics and Mechanics 24 (2015) 242-252 Received: November 3, 2015

STRUCTURAL VARIATIONS IN LOW-CARBON STEEL UNDER SEVERE PLASTIC DEFORMATION BY DRAWING, FREE TORSION, AND DRAWING WITH SHEAR

G.I. Raab[1,2], D.V. Gunderov[1,2], L.N. Shafigullin[1], Yu.M. Podrezov[3], M.I. Danylenko[3], N.K. Tsenev[4], R.N. Bakhtizin[4], G.N. Aleshin[1,2], A.G. Raab[2*]

[1]Kazan Federal University, Kremlyovskaya st. 18, Kazan, 420000, Russia

[2]Ufa State Aviation Technical University, Karl Marx st. 12, Ufa, 450000, Russia

[3]Frantsevich Institute for Problems in Materials Science NASU, Krzhizhanovsky st. 3, Kiev, 03680, Ukraine

[4]Ufa State Petroleum Technical University, Kosmonavtov st. 1, Ufa, 450062, Russia

*e-mail: agraab@mail.ru

Abstract. This paper presents the findings of the numerical simulation of conventional drawing, free torsion and drawing with shear, as well as the structural studies of deformed billets fabricated of low-carbon steel. The non-uniform severe deformation distribution observed in the model corresponds principally to actual physical experiments with similar parameters of structural inhomogeneity. It has been found that the diffusion processes of dissolution of the initial dispersed cementite particles and formation of new ones become essentially more active. The microhardness of Steel 10 rod surface layer therewith increases up to ~ 7000 MPa.

1. Introduction

Severe plastic deformation (SPD) is one of the most efficient tools to enhance the complex of physical and mechanical properties of metal materials by structure refinement down to ultrafine-grained (UFG) and nanocrystalline (NC) states [1, 2]. The patterns of deformation processing generally used to form UFG and NC structures are high-pressure torsion, equal-channel angular pressing, screw extrusion, etc. [3–5]. Although loading conditions in the patterns are rather different, the structure refinement in all the cases takes place due to active shear strain in the constrained environment under the joint action of tension and compression. Further development of SPD techniques implies the creation of combined loading patterns necessarily including the shear strain component.

The most widely known and popular pattern of a pure shear is free torsion [6]. By combining with the reduction pattern applied during drawing, one can disperse the structure of long metal semi-finished products and, as a result, to enhance the complex of mechanical properties. In recent years, the authors have been elaborating upon this type of strain treatment, which is labelled as the drawing with shear [7-10]. Due to its high capacity comparable to that of conventional drawing, drawing with shear can be used to produce UFG wire and rods on commercial scale.

This paper sets the task of comparing the effect of drawing with shear, conventional drawing and free torsion on strain intensity and corresponding variations in structure taking place in low-carbon steel processed by these types of treatment. Also, the interdependence of

these variations with mechanical characteristics is considered.

To meet this challenge, numerical simulation was used to evaluate the distribution of severe plastic deformation. The work performed made it possible to compare simulation results with the observed variations in structure and properties of materials.

2. Material and experimental procedures

Low-carbon steel in as-delivered state in the form of a calibrated rod of 10 mm in diameter was used as a research material. The chemical composition of the steel is shown in Tab. 1.

Table 1. Chemical composition of the low-carbon steel under investigation.

%, weight									
C	Si	Mn	S	P	Cr	Ni	As	N	Cu
0.12	0.29	0.41	0.01	0.02	0.04	0.03	0.01	0	0.05

When developing a numerical model, the flow characteristics of Steel 10 were selected in compliance with the recommendations given in paper [11].

A typical software package DEFORM-3D was used to implement numerical simulation process. Prior to the simulation, 3-D models were created in Compas-3D application.

The following assumptions were made regarding the models of drawing, free torsion and drawing with shear:

1) The starting stock is ductile and isotropic.
2) The temperature of strain environment is 20 ºC.
3) The instrument is rigid.
4) The diameter of starting stock is 10 mm and length is 250 mm.
5) Drawing (and drawing with shear) simulation included 150 steps embracing the full cycle of billet processing in forming dies.
6) Torsion simulation included 180 steps with a time interval of 1 sec and a rotational speed of 12.5 r/min.
7) The billet is subdivided into 55,000 trapezoidal elements.
8) The coefficient of friction between a billet and the instrument calculated from the Siebel's formula equals to 0.12.
9) Drawing speed is 0.95 mm/sec.
10) One-pass strain degree equals to 15%.
11) Rotational rate of a moving forming dye is 500 min^{-1}.

The simulation results were used to determine the intensity variations in cumulative plastic deformation Λ_m along the cross-section diameter of billets treated by deformational processing.

Physical experiment. The physical experiment included three types of strain treatment for steel 10 rods, namely conventional drawing, free torsion, and drawing with shear [7-10, 12-15].

Conventional drawing was implemented in several passes through conical forming dies of the drawing bench with a starting force of 30 kN and the initial rod working length of 200 mm with a gradual diameter decrease from 10 to 6.6 mm (Tab. 2).

Free torsion was performed using the turning machine with a cantilever fixation of both billet parts in moving and stationary die heads varying the number of rotations from 10 to 30.

Drawing with shear included the reduction treatment combined with a shear. The propelling force was applied during tandem drawing through conic drawing dies and simultaneous rotation of one of the dies [7-10]**.** Deformation processing included rotation of a drawing die contributing to additional shear strain. An eccentricity formed by a conic die channel is specified about the rotation axis (Fig. 1).

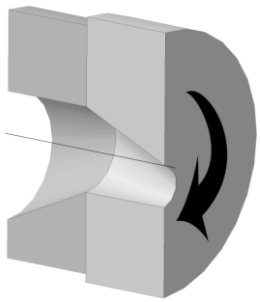

Fig. 1. 3-D model of drawing with shear dies

Drawing with shear (one pass) was performed using a drawing bench with an extension for die rotation. Diameter of dies reduced from 0 to 9.5 mm in a single pass. The selected loading patterns enable to further analyze structural and strength variations when implementing three different strain patterns, namely, compression with shear (during drawing), pure shear (during free torsion), and compression with shear and rotation (during drawing with shear). In the latter case, the role of shear strain is considerably greater than during conventional drawing.

During the study of deformed samples, the efficiency of the strain effect on the structure under various treatment conditions was compared. Variations in cumulative deformation intensity $\mathbf{\Lambda_m}$ along cross-sectional diameter of **D** rods during simulation were calculated from diagrams of $\mathbf{\Lambda_m}$ dependency on **D**.

The value of drawing strain $\boldsymbol{\varepsilon}$ was calculated by the following formula within the physical experiment:

$$\varepsilon = [(S_o - S_1)/S_o] \times 100\%, \quad (1)$$

where S_o is the area of a rod cross section prior to drawing, and S_1 is the area after drawing [14-17].

Metallographic examinations of the material structure both in the initial and the deformed states were conducted using Olympus light microscope, JEOLJSM-6390 raster microscope and JEM-2100 scanning microscope. Mean grain size, features of cell and dislocation structures of ferrite and cement carbide materials, the pattern of microcracks' location, as well as the morphology and distribution of Fe_3C particles were investigated in compliance with [18]. Furthermore, HV microhardness was measured under a load of 1 H and during a holding time of 10 sec in the cross section of rods prior and after deformation. The measuring error of the values mentioned didn't surpass 8 %.

3. Experimental results and discussion

Drawing. Relying on the findings of mathematical simulation of the drawing process, the strain intensity $\mathbf{\Lambda_m}$ was determined along the rod diameter. For illustration purposes, the graphical representation of the rod is shown in Fig. 2. It is obvious from the graph that the distribution of strain intensity following conventional drawing is rather uniform, with only slight variation in $\mathbf{\Lambda_m}$ from the periphery to the center of the sample (from ≈ 0.9 to ≈ 0.95). So, this indicates the "conservative" nature of conventional drawing pattern.

Free torsion. The simulation pattern of the distribution of cumulative deformation intensity both along the surface and in the cross section of a rod processed via free torsion (16 rotations) suggests that strain degree Λ increases nonlinearly from $\mathbf{\Lambda_m} \approx 0.5$ in the center up to $\mathbf{\Lambda_m} \approx 2.3$ in the periphery of the rod. This seems typical of torsion strain development [15, 17]. Such a non-uniform distribution $\mathbf{\Lambda_m}$ in radial axis was described in the paper [17]. It was observed when applying free torsion to cylindrical samples fabricated of the Ti alloy VT 6.

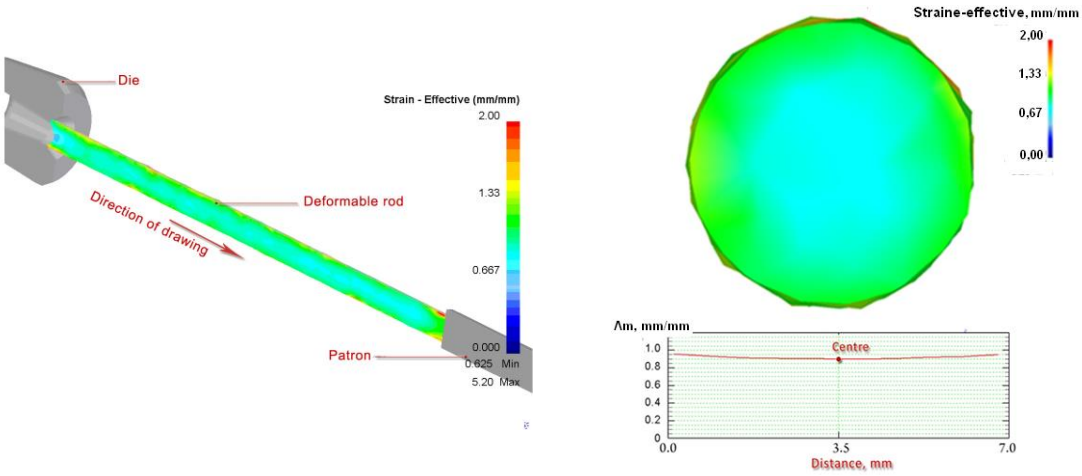

a) b)

Fig. 2. Mathematical simulation of strain intensity distribution Λ_m during drawing of Steel 10 rods for 5 passes: a) the general view of the deformed rod, steady state, longitudinal section; b) variations in Λ_m along the cross section of the rod diameter.

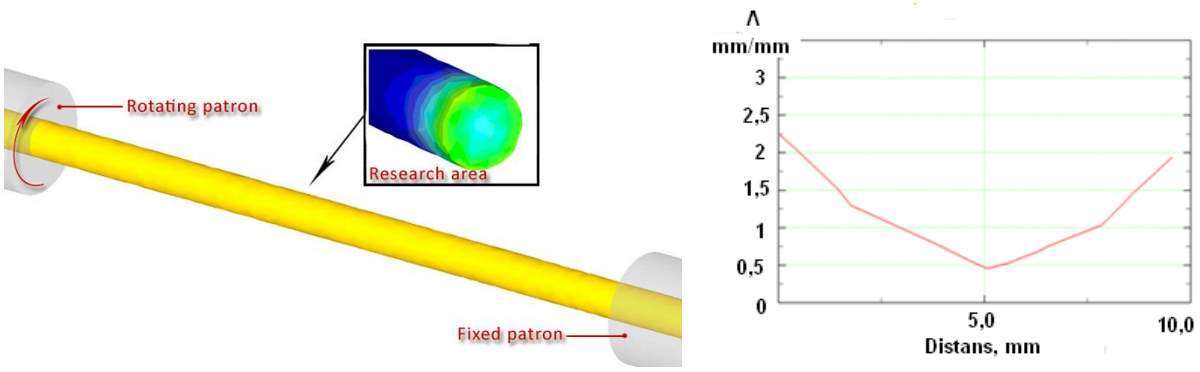

a) b)

Fig. 3. Mathematical simulation of strain intensity distribution Λ_m in the cross section of the sample processed via free torsion (16 revolutions): general view (a), and Λ_m variation along the diameter of the sample (b).

Drawing with shear. Drawing with shear process was simulated using DEFORM-3D and is schematically shown in Pic. 4. As the figure suggests, a typical feature of drawing with shear is a spiral variation in the intensity of cumulative plastic deformation along a Steel 10 rod. It should be noted that helical deformation bands were found on the surface of rods processed via drawing within the physical experiment as well.

As indicated by the computer simulation, Λ_m equals 0.2 and 0.95 after conventional drawing in 1 and 5 passes, correspondingly (with comparatively uniform strain distribution throughout the rod (Pic. 2)). At the same time, a one-pass drawing with shear resulted in a distinctly non-uniform distribution of strain intensity, increasing from the center to the periphery of the rod, with Λ_m achieving up to about 2.7 in the near-surface region (Pic. 5, Tab. 2). This points to the fact that strain is more intense while processing by drawing with shear, which is connected with the geometry of forming dies and the method of their rotation relative the drawing axis. Hence even once cycle of drawing with shear results in much higher levels of strain intensity, and, consequently, higher productivity when fabricating long high-strength products. At the same time, the drawing force and the normal force of the instrument are decreased by almost 2 and 1.8 times, correspondingly, as compared to torsion-free drawing [7, 8].

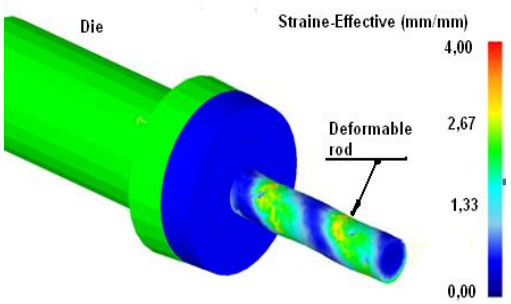

Fig. 4. Drawing with shear and a spiral variation in the intensity of cumulative plastic deformation on Steel 10 rod surface.

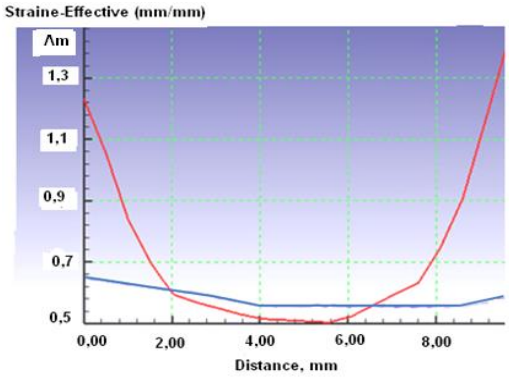

Fig. 5. Mathematical simulation of strain intensity distribution Λ_m after deformation by conventional drawing for 2 passes —— and drawing with shear for 1 pass —— along the cross section of the rod diameter.

Table 2 shows the intensity of cumulative deformation **(Λ_m)** during the simulation of the specified types of processing.

Table 2. Deformation processing conditions of Steel 10 rods.

Drawing				Free torsion (**Ø = Ø$_o$**)			Drawing with shear, 1 cycle	
N_d	**Ø**, mm	**ε, %**	**Λ_m**	**N_r**	Centre **Λ_m^c**	Periphery **Λ_m^p**	**Λ_m^{min}**	**Λ_m^{max}**
1	9.2	15	0.2	10	0.2	1.1	**0.5**	**2.7**
2	8.4	29	0.5	16	0.4	2.3		
3	7.6	42	0.75	22	0.7	3.4		
4	7.0	50	0.9	-	-	-		
5	6.5	56	0.95	-	-	-		

N_d - number of drawing passes; **Ø** – diameters of rods after corresponding number of drawing passes; **ε** – degree of strain by drawing, calculated by formula 1; **N_r**.– number of free torsion revolutions; initial rod diameter **Ø$_o$** = 10 mm, **t_{def}** =20 ºC

Among other things, Tab. 2 shows that **Λ_m^{max}** of 2.7 measured in certain points of a rod processed via one-cycle drawing with shear exceeds **Λ_m^p** 0f 2.3 observed on a rod surface processed via 16 revolutions of free torsion. To estimate the findings of numerical simulation, full-scale experiments on conventional drawing, free torsion and drawing with shear were conducted according to the techniques described above subject to the processing conditions taken for the pattern.

In order to reveal the features of plastic deformation throughout the deformed rods,

microhardness HV was measured along the cross-sectional diameter of rods. The graphs for such measurements are shown in Fig. 6.

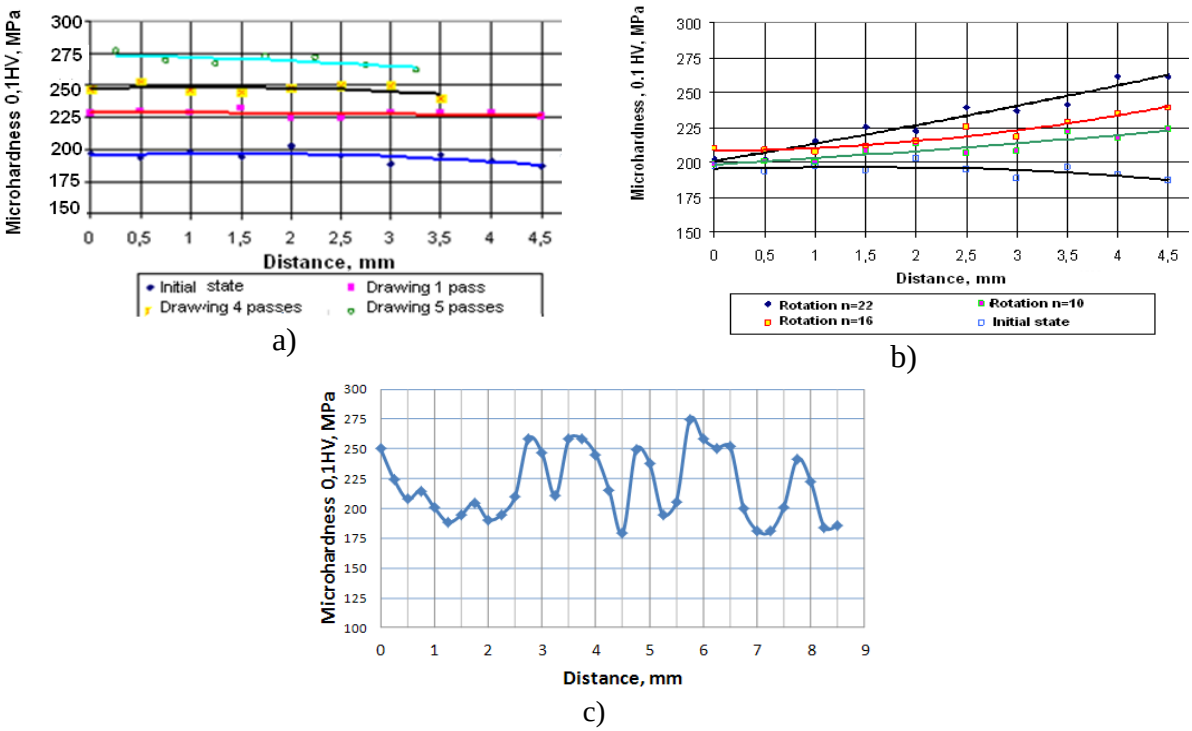

Fig. 6. Variations in microhardness along the cross-sectional diameter of Steel 10 rods processed via: a) drawing; b) free torsion; c) drawing with shear. Physical experiment.

As can be seen from the shown graphs, microhardness of initial Steel 10 rods in the center and the periphery is much the same. Conventional drawing with the increase in strain degree (in the number of passes) results in almost uniform enhancement of HV values along the whole rod section (Fig. 6a). This points to the comparatively uniform nature of drawing strain throughout rods, substantiated by the structural research findings. The presented data principally correspond to the simulation results and suggest the correlation between strain intensity and microhardness.

Unlike drawing, torsion strain leads to non-uniform microhardness variations (Fig. 6b). Microhardness in central parts of rods subjected to torsion remains at the initial level, while in the periphery Hv values considerably increase. Such a pattern of microhardness variation corresponds to the results shown in paper [18], considering the torsion with simultaneous extension of Steel 10 rods. And this is directly connected with non-uniformity of pure shear stress induced by torsion [17]. It should be noted that HV values (at the edge points) during free torsion with much higher Λ_m^p = 3,4 (Nr. = 22) achieve nearly the same level (2.7) as during conventional drawing treatment with Λ_m.=0.95 (56 %). This result is subject to further confirmatory investigations and analysis.

Variations of microhardness values observed along the whole cross section of rods during drawing with shear processing are even more non-uniform and stepwise (Fig. 6c). However, this doesn't correspond to the pattern of strain intensity variation along the cross-sectional diameter developed by simulation (Fig. 5). On the other hand, it is worth noting that such a stepwise variation of HV along the cross-sectional diameter of rods (Pic. 6c) may reflect to a certain degree a spiral variation of the cumulative plastic deformation (Figs. 4 and 6c). As noted above, the simulated spiral variation of the cumulative deformation intensity corresponds to helical deformation bands observed during the physical experiment on the surface of rods processed via drawing with shear.

Microhardness was measured directly at the surface of rods within the mentioned bands with unusual results obtained. HV constituted about 7,000 MPa, which far exceeds the maximum HV values in cross sections of deformed rods. The found features of strain effect on the type of structure formed (which can be regarded as a gradient one) reveal an increasingly important role of shear deformation during drawing with shear as compared to the conventional drawing.

Variations in microhardness caused by the increase in deformation intensity are verified by metallographic investigations. Figures 7-8 show the microstructural images of Steel 10 rods in the initial state and after deformation processing.

Figure 7a demonstrates predominantly equiaxed ferrite grains with relatively straight-line boundaries and a mean grain size of $d_{cp.} \approx$ 12-13 μm along the whole cross-sectional area of rods. Rounded particles of degenerated perlite Fe_3C of an indefinite shape with $d_{Fe3C} \approx$ 0.2-3.0 μm and frequently stretched into chains are randomly distributed along ferrite grain boundaries.

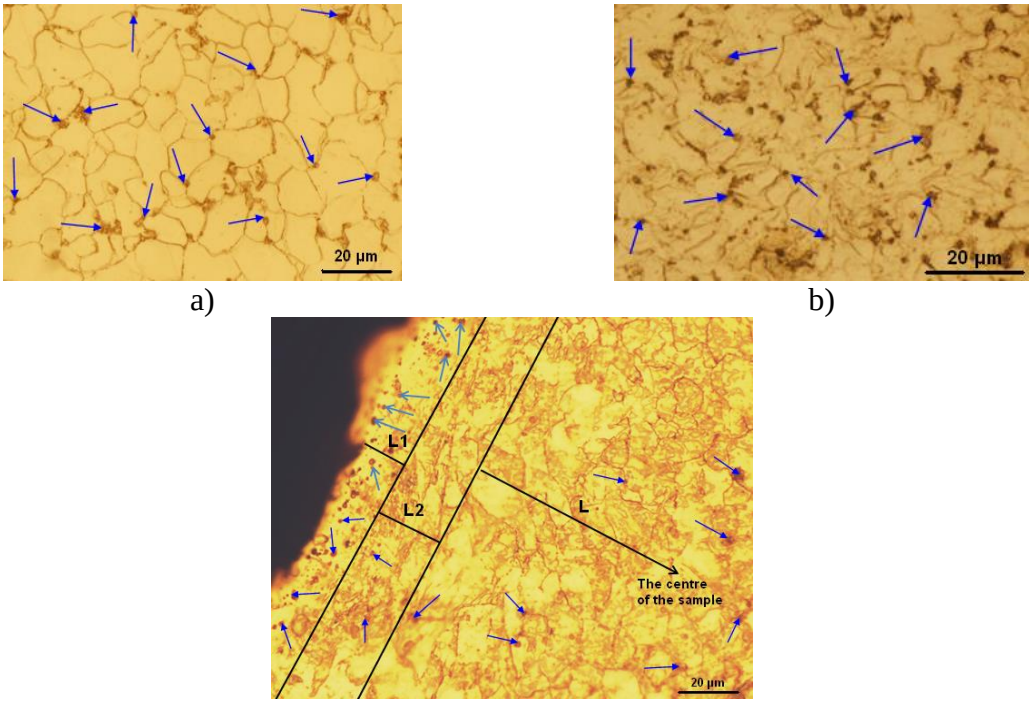

Fig. 7. Microstructure of Steel 10: a) initial state; b) the rod central area subjected to 5 drawing passes; c) gradient microstructure of the sample periphery upon drawing with shear. L_1 is a strongly deformed near-surface area of about 20 μm in width, L_2 is a transition region of about 30 μm in width. The areas with various types of deformation (L_1, L_2, L) are conventionally divided with lines. Blue arrows point to some Fe_3C cementite particles (of degenerated perlite). Light microscopy.

When studying the cross-sectional structure of deformed rods subjected to 5 passes of the conventional drawing, it was established that the alloy structure was relatively homogeneous with non-equiaxed, strongly deformed, frequently bended grains (of ferrite). The boundaries were curved, and the grain size d_3 was about 7.5 μm (Fig. 7b). Generally, microstructure of the center and the periphery of rods is identical. The pattern of distribution and size of perlite particles remained nearly the same.

Somewhat different situation is observed in the alloy samples processed via torsion. Both ferrite grains and perlite particles located in the center of the free torsion processed rod remained of nearly the same size. Also, the structure contains randomly distributed deformed

ferrite grains. At the same time, peripheral areas of rods demonstrate predominantly deformed ferrite grains with curved boundaries like those shown in Fig. 7b. Besides, single microcracks appear even after 16 revolutions of torsion mainly at interphase boundaries of the periphery of samples close to the side surface of rods (note that even after of drawing with shear no cracks were seen). After 22 revolutions of torsion microcracks are observed throughout rods (Fig. 8). So, free torsion is a more "rough" deformation processing as compared to the conventional drawing due to high intensity of defect accumulation resulting in microcrack propagation and further sample destruction.

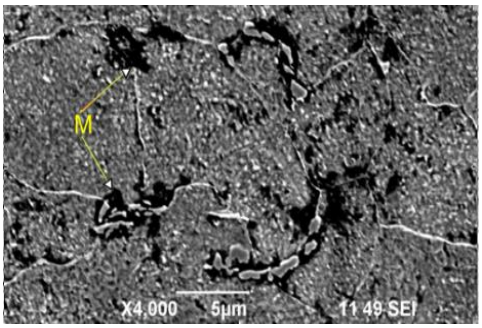

Fig. 8. Torsion strain, 22 revolutions, the central part of a rod, SEM, M – microcracks at interphase boundaries.

TEM studies of thin foils revealed misoriented cells located in deformed ferrite grains throughout rods processed via drawing. As a rule, such cells are elongated along drawing direction and have dimensions of about 0.3-0.5 μm in width and about 1-3 μm in length.

Elongated cells are also observed in the periphery of samples processed via free torsion for 16 revolution. However, such cells have larger misorientations as compared to drawing processing as evidenced by both azimuthal scatter and spot reflections on electron-diffraction patterns. Also, cells in the periphery of samples processed via torsion are of smaller size than the ones subjected to drawing, with the width of no more than 0.2-0.3 μm, and the length of no more than 0.5-1 μm (Fig. 9).

Unlike the periphery, the central part of torsion-processed samples contains slightly misoriented cells of an arbitrary shape (Fig. 7a). This suggests that cumulative deformation of the central part of samples after torsion is less intense, which corresponds to the microhardness measurements and simulation findings.

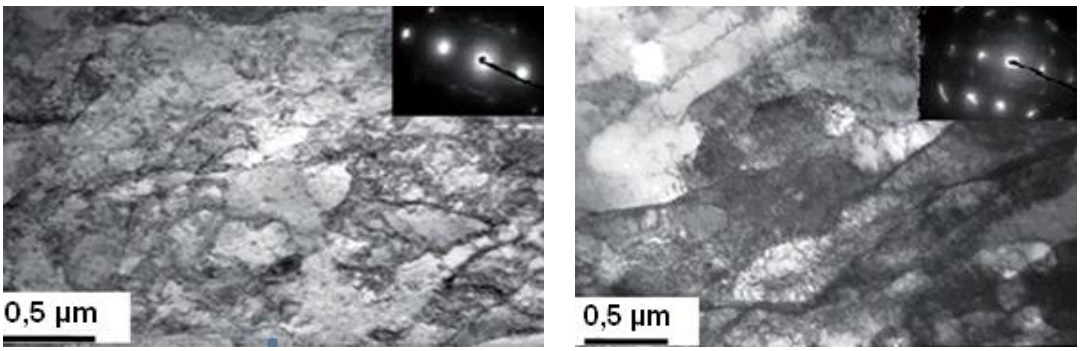

a) b)

Fig. 9. TEM images of the microstructure of Steel 10 samples deformed with free torsion: a) the central part of a rod, zone [111] axis; b) the periphery of a rod zone [110] axis.

Special attention should be paid to studying the microstructure of steel processed by drawing with shear. Distinctly non-uniform distribution and morphology of ferrite grains and Fe_3C particles are observed in the cross-section of a rod subjected to this type of treatment

(Pic. 7c). Volume fraction and distribution of cementite particles in the central region (region L in Pic. 7c) with relatively low deformation after drawing with shear are nearly similar to those after one-pass conventional drawing. At the same time, it is not the case with the periphery of a rod. The so-called transition region with fiber structure is composed of strongly elongated curved ferrite grains (region L_2 in Pic. 7c) with no cementite particles observed. The strongly deformed subsurface region of a rod (region L_1 in Pic. 7c) yet contains a number of fine Fe_3C particles of about 0.1 ÷ 0.4 μm in size of highly non-uniform distribution density. Some areas of subsurface rod region have no cementite particles, while other areas mostly contain particles with the density of two or three times as much as in the central rod region. This is typical of the whole subsurface and transition regions of the cross-section of rods processed via drawing with shear.

The observed microstructural variations as to the size and distribution pattern of cementite particles point to the activation of the diffusion processes of dissolution of initial Fe_3C particles with further formation of new cementite particles in a strongly deformed subsurface region of a rod (region L_1) processed via drawing with shear. It should be noted that the found activation of cementite initial particles is observed in a transition region (region L_2 in Pic. 7c) of a rod cross-section only.

Basing on the increasing number of disperse Fe_3C particles in L_1 region, it can be assumed that an active interaction of deformation defects with existing Fe_3C particles takes place during severe plastic deformation in a subsurface region of rods. This results in an intense cementite decomposition. According to [12-22], this destruction begins with the outflow of carbon atoms from carbide following the interaction with deformation defects, which results in the formation of non-stoichiometric cementite being thermodynamically unstable. This appears to be the main reason for cementite dissolution.

Carbon atoms released after cementite decomposition precipitate in dislocations as well as at grain and cell boundaries, forming numerous agglomerates (segregations) on these defects. Then, new Fe_3C particles are formed from these segregations.

Similar cementite dissolution during SPD was also observed in papers [19-23]. Local oversaturation of ferrite with carbon takes place due to such dissolution of Fe_3C particles. Such a non-equilibrium oversaturation of cementite with carbon results in the formation of numerous Fe_3C disperse precipitations. It is known that the process of precipitation formation [24] is thermally activated. So, new cementite precipitations are formed in a subsurface region (region L_1) heated most during drawing with shear (for at least 170 ^oC! [25]). As a result, carbon concentration in the specified area of cementite decreases and becomes equilibrium. The formation of gradient causes an active diffusion of carbon atoms from oversaturation areas (region L_2) during interaction with dislocations and vacancies, as well as at grain and subgrain boundaries into L_1 region, where they are absorbed by newly formed Fe_3C particles. This process is somewhat similar to the coalescence of secondary phase particles of alloys, while larger precipitates increase at the expense of the dissolution of smaller ones [21, 22, 24, 26]. Obviously, such a “transfer” of carbon atoms from L_2 to L_1 region results in the decrease in solute carbon atom concentration down to an equilibrium state, which eliminates the cause for the formation of new cementite particles in L_2 transition region. This can be viewed as the reason for the absence of both initial and new Fe_3C precipitates in this region of Steel 10 microstructure cross-section processed via drawing with shear.

The observed structural variations are inhomogeneous in nature, which is connected with the distribution of cementite particles in the cross section of a rod. To a certain degree, this is correlated with non-uniformity of microhardness values observed along the cross-sections radius of a rod. Higher than normal microhardness on the surface of rods subjected to drawing with shear is, on the one hand, caused by high density of disperse cementite precipitations in L_1 region, grain, subgrain boundaries, dislocation and other structural

defects, and on the other hand by carbon atom segregations formed at ferrite grain boundaries.

As mentioned above, the establishment of direct correlation between the parameters of deformation process simulation and structural variations in deformed alloys provides a means for implementation of new approaches to the development and management of deformation processing of metal materials aimed at structure refinement and formation of the specified complex of physical and mechanical properties.

It was found that free torsion led to a considerable structure inhomogeneity and a gradient of mechanical properties from the central part to a surface of a rod both during the simulation and the physical experiment.

On the whole, the results obtained suggest that drawing with shear is the most promising method of deformation processing to further enhance the complex of service properties of long products [6-9]. It is conceivable that the given pattern gives the possibility to implement the advantages of conventional drawing and free torsion with higher efficiency.

4. Conclusions

1. Various types of cold deformation processing were applied to rods fabricated of low-carbon steel, namely, conventional drawing and free torsion. A considerable non-uniformity of structural variations and patterns of SPD distribution was observed under deformation.

2. It has been shown that as a result of deformation by conventional drawing the structure is processed more uniformly, which leads to more stable change of microhardness HV throughout a rod. Free torsion processing leads to a uniform increase in HV from the center to the periphery of a rod. At the same time, drawing with shear results in the formation of structure with high level of inhomogeneity with regular erratic HV jumps within the regions of 300-500 μm in size.

3. It has been demonstrated that simulation of conventional drawing, free torsion and drawing with shear mainly corresponds to the findings of the physical experiment with similar deformation parameters. This confirms the correctness of approaches applied as well as the promising nature of mathematical simulation for the development and improvement of new metal pressure forming procedures.

4. It has been established that during drawing with shear a gradient structure is formed, which increases the microhardness of the surface layer up to values close to 7000 MPa. Also, strain-induced cementite dissolution occurs during cold plastic deformation of low-carbon steel.

5. It has been shown that during drawing with shear, the diffusion processes of dissolution of the initial dispersed cementite particles and formation of new ones become essentially more active, due to the interaction of such particles with defects of dislocation origin.

Acknowledgments

G.I. Raab, D.V. Gunderov and L.N. Shafigullin acknowledge gratefully the funding through the Russian Government Program of Competitive Growth of Kazan Federal University.

A.G. Raab gratefully acknowledges the financial support of the Russian Science Foundation grant (Project № 15-19-0144) allocated to Ufa State Aviation Technical University for conduction of computer modeling and manufacturing of deforming tool for physical experiment.

Yu.N. Podrezov, M.I. Danylenko, R.N. Bakhtizin and N.K. Tsenev would like to acknowledge the support from the Ukraine-Russian Science Foundation grant (project Ukr_a 0890429), allocated to Ufa State Aviation Technical University.

G.N. Aleshin acknowledge gratefully the financial support from the Ministry of Education and Science of Russia through project No. 11.729.2014K.

References

[1] R.Z. Valiev, A.P. Zhilyaev, T.G. Langdon, *Bulk Nanostructured Materials: Fundamentals and Applications* (Wiley STM, USA, 2014).

[2] R.Z. Valiev, O.A. Kaibyshev, R.I. Kuznetsov, R Sh. Musalimov, N.K. Tsenev // *Doklady Akademii Nauk USSR* **301(4)** (1988) 864. (In Russian).

[3] R.Z. Valiev, I.V. Alexandrov, *Bulk nanostructured metal materials: production, structure and properties* (Academkniga Publishing Book-Trading Center, Moscow, 2007).

[4] O.A. Kaibyshev, F.Z. Utyashev *Superplasticity, structure refinement and processing of hard-to-deform alloys* (Nauka, Moscow, 2002). (In Russian).

[5] Ya.Yu. Beygelzimer, V.N. Varyukhin, D.V. Orlov, S.G. Synkov, *Screw extrusion: deformation accumulation process* (TEAN Company, Donetsk, 2003).

[6] M.A. Borodin, *Strength of materials* (Drofa, Moscow, 2001). (In Russian).

[7] G.I. Raab, A.G. Raab // *Patent No. 2347633* as of November 12, 2007.

[8] G.I. Raab, A.G. Raab // *Izobretateli – mashinostroyeniyu* **3** (2011) 4. (In Russian).

[9] M.V. Chukin, A.G. Raab, V.I. Semenov, I.R. Aslanian, G.I. Raab // *Journal of the MSTU named after G.I. Nosov (Magnitogorsk)* **4** (2012).

[10] G.I. Raab, A.G. Raab // *Patent No. 2347633 RF*, 27.02.2009.

[11] V.G. Sorokin, A.V. Volosnikova, S.A. Vyatkin, *Steel and alloy grade guide* (Mashinostroyenie, Moscow, 1989). (In Russian).

[12] I.L. Perlin, M.Z. Yermanok, *Drawing theory* (Metallurgy, Moscow, 1971). (In Russian).

[13] V.L. Kolmogorov, *Mechanics of pressure metal treatment* (UPI, Ekaterinburg, 2001). (In Russian).

[14] A.N. Levanov, V.L. Kolmogorov, S.P. Burkin, B.R. Kartak, *Contact friction within pressure metal treatment* (Metallurgy, Moscow, 1976) 416. (In Russian).

[15] D.G. Verbilo // *Strength problems* **3** (2011) 110.

[16] S.A. Saltykov, *Stereometric metallography* (Metallurgy, Moscow, 1976) 273. (In Russian).

[17] V.K. Berdin // *USATU Journal. Engineering technology* **15(4)** (2011) 175.

[18] E.G. Pashinskaya, I.I. Tischenko, V.V. Stolyarov, M.A. Kralyuk // *Naukovy Notatki* **25** (2009) 182.

[19] V.Y. Tsellermaer // *Steels in Translation* **29 (**1999) 75.

[20] N.I. Danilenko, V.V. Kovylyaev, S.S. Ponomaryov, S.A. Firstov // Naukovy Notatki **69** (2009) 72.

[21] Yu.Yu. Efimova, N.V. Koptseva, O.A. Nikitenko // *Journal of the MSTU named after G.I. Nosov (Magnitogorsk)* **4** (2009) 45.

[22] Yu. Ivanisenko, I. MacLaren, X. Sauvage, R.Z. Valiev, H.-J. Fecht // *Solid State Phenomena* **114** (2006) 133.

[23] Y.G. Ko, D.H. Shin, In: *Nanostructured Metals and Alloys: Processing, Microstructure, Mechanical Properties and Applications*, ed. by S.H. Whang (Woodhead Publishing Limited, 2011), p. 243.

[24] I.I. Novikov, *Theory of metal thermal treatment* (Metallurgy, Moscow, 1986). (In Russian).

[25] F.Z. Utyashev, G.I. Raab, *Deformation Methods for Fabrication and Processing of Ultrafine-Grained and Nanostructured Materials* (Gilem, Ufa, 2013).

[26] J.W. Martin, R.D. Doherty, *Stability of Microstructure in Metallic Systems* (Atomizdat, Moscow, 1978). (In Russian. Translated from English).